



**Universiteit
Leiden**
The Netherlands

RIPK1 expression associates with inflammation in early atherosclerosis in humans and can be therapeutically silenced to reduce NF- κ B activation and atherogenesis in mice

Karunakaran, D.; Nguyen, M.A.; Geoffrion, M.; Vreeken, D.; Lister, Z.; Cheng, H.S.; ... ; Rayner, K.J.

Citation

Karunakaran, D., Nguyen, M. A., Geoffrion, M., Vreeken, D., Lister, Z., Cheng, H. S., ... Rayner, K. J. (2021). RIPK1 expression associates with inflammation in early atherosclerosis in humans and can be therapeutically silenced to reduce NF- κ B activation and atherogenesis in mice. *Circulation*, 143(2), 163-177. doi:10.1161/circulationaha.118.038379

Version: Publisher's Version
License: [Creative Commons CC BY-NC-ND 4.0 license](#)
Downloaded from: <https://hdl.handle.net/1887/3195267>

Note: To cite this publication please use the final published version (if applicable).

RIPK1 Expression Associates With Inflammation in Early Atherosclerosis in Humans and Can Be Therapeutically Silenced to Reduce NF- κ B Activation and Atherogenesis in Mice

BACKGROUND: Chronic activation of the innate immune system drives inflammation and contributes directly to atherosclerosis. We previously showed that macrophages in the atherogenic plaque undergo RIPK3 (receptor-interacting serine/threonine-protein kinase 3)-MLKL (mixed lineage kinase domain-like protein)-dependent programmed necroptosis in response to sterile ligands such as oxidized low-density lipoprotein and damage-associated molecular patterns and that necroptosis is active in advanced atherosclerotic plaques. Upstream of the RIPK3-MLKL necroptotic machinery lies RIPK1 (receptor-interacting serine/threonine-protein kinase 1), which acts as a master switch that controls whether the cell undergoes NF- κ B (nuclear factor κ -light-chain-enhancer of activated B cells)-dependent inflammation, caspase-dependent apoptosis, or necroptosis in response to extracellular stimuli. We therefore set out to investigate the role of RIPK1 in the development of atherosclerosis, which is driven largely by NF- κ B-dependent inflammation at early stages. We hypothesize that, unlike RIPK3 and MLKL, RIPK1 primarily drives NF- κ B-dependent inflammation in early atherogenic lesions, and knocking down RIPK1 will reduce inflammatory cell activation and protect against the progression of atherosclerosis.

METHODS: We examined expression of RIPK1 protein and mRNA in both human and mouse atherosclerotic lesions, and used loss-of-function approaches in vitro in macrophages and endothelial cells to measure inflammatory responses. We administered weekly injections of RIPK1 antisense oligonucleotides to *ApoE*^{-/-} mice fed a cholesterol-rich (Western) diet for 8 weeks.

RESULTS: We find that RIPK1 expression is abundant in early-stage atherosclerotic lesions in both humans and mice. Treatment with RIPK1 antisense oligonucleotides led to a reduction in aortic sinus and en face lesion areas (47.2% or 58.8% decrease relative to control, $P < 0.01$) and plasma inflammatory cytokines (IL-1 α [interleukin 1 α], IL-17A [interleukin 17A], $P < 0.05$) in comparison with controls. *RIPK1* knockdown in macrophages decreased inflammatory genes (NF- κ B, TNF α [tumor necrosis factor α], IL-1 α) and in vivo lipopolysaccharide- and atherogenic diet-induced NF- κ B activation. In endothelial cells, knockdown of *RIPK1* prevented NF- κ B translocation to the nucleus in response to TNF α , where accordingly there was a reduction in gene expression of *IL1B*, *E-selectin*, and monocyte attachment.

CONCLUSIONS: We identify RIPK1 as a central driver of inflammation in atherosclerosis by its ability to activate the NF- κ B pathway and promote inflammatory cytokine release. Given the high levels of RIPK1 expression in human atherosclerotic lesions, our study suggests RIPK1 as a future therapeutic target to reduce residual inflammation in patients at high risk of coronary artery disease.

Denuja Karunakaran¹,
PhD

Katey J. Rayner², PhD

The full author list is available on page 175.

Key Words: atherosclerosis
■ inflammation ■ macrophages ■ NF- κ B
■ RIPK1 protein, human

Sources of Funding, see page 176

© 2020 American Heart Association, Inc.

<https://www.ahajournals.org/journal/circ>

Clinical Perspective

What Is New?

- RIPK1 (receptor-interacting serine/threonine-protein kinase 1) acts as a proinflammatory hub in the vessel wall, with increased expression and coincident activation of NF- κ B (nuclear factor κ -light-chain-enhancer of activated B cells) in early atherosclerotic disease in humans.
- Reducing RIPK1 expression in mice prevents atherosclerosis development, in part, by reducing endothelial and macrophage activation of inflammatory pathways, including interleukin 1 α and interleukin 1 β .

What Are the Clinical Implications?

- Inflammation as a therapeutic target for atherosclerotic vascular disease was recently validated by the CANTOS trial (Cardiovascular Risk Reduction Study [Reduction in Recurrent Major CV Disease Events]), and we identify herein that the therapeutic silencing of RIPK1 acts as a parallel but alternative strategy to dampen inflammation in the vessel wall.
- Antisense oligonucleotides can effectively decrease RIPK1 expression and activation without the unwanted spontaneous activation of inflammatory cell death that accompanies complete loss of RIPK1, making this approach readily translatable to human disease.

Atherosclerosis begins as an innate immune response to modified cholesterol-rich lipoproteins trapped in the subendothelial space of the vessel wall, recruiting inflammatory monocytes from the circulation.^{1,2} These monocytes differentiate into macrophages that avidly engulf modified lipids (eg, oxidized low-density lipoprotein) through scavenger receptors (eg, CD36, SR-A) to become foam cells. Although these foam cells initially play a protective role in mediating the efflux of cholesterol from the lesions, they also engage the NF- κ B (nuclear factor κ -light-chain-enhancer of activated B cells) pathway to transcriptionally activate the production of proinflammatory cytokines (eg, TNF α [tumor necrosis factor α], GM-CSF [granulocyte-macrophage colony-stimulating factor], IL-1 α/β [interleukin 1 α/β]), and chemokines to sustain the local inflammatory environment, resulting in additional monocyte recruitment.³ Furthermore, double-hit engagement by modified lipoproteins and other sterile inflammatory cues (eg, ATP) can trigger NF- κ B–regulated NLRP3 (NLR family pyrin domain containing 3) inflammasome-dependent IL-1 β (interleukin 1 β)⁴ or inflammasome-independent and oxidative stress–dependent IL-1 α (interleukin 1 α) secretion.⁵ As foam cells become overwhelmed with lipid, they can undergo cell death. To date, several

types of cell death pathways have been identified to occur with atherosclerotic lesions: noninflammatory apoptosis, proinflammatory necroptosis, and secondary necrosis.^{6–10} The ineffective clearance of these dying macrophages by efferocytosis adds to the lesional burden, forming a large necrotic core that destabilizes the atherosclerotic plaque.^{11,12} In the past 3 decades, low-density lipoprotein (LDL)–lowering therapies have emerged as the leading therapeutic strategy to successfully prevent or treat atherosclerosis. Although such therapies are highly effective, they reduce atherosclerotic disease incidence by only 50% to 60%, leaving considerable residual disease burden.¹³ Moreover, with the recent failures of high-density lipoprotein–raising therapies as an alternative therapeutic approach,¹⁴ there is renewed focus in finding novel therapeutic targets that act in parallel with cholesterol-lowering drugs to eliminate residual inflammation within lesions. The outcomes of 2 large clinical trials targeting inflammation in coronary artery disease, CANTOS (Cardiovascular Risk Reduction Study [Reduction in Recurrent Major CV Disease Events]),¹⁵ which used an IL-1 β monoclonal antibody, and COLCOT (Colchicine Cardiovascular Outcomes Trial),¹⁶ which used low-dose anti-inflammatory colchicine; both demonstrated reduced cardiovascular events in high-risk patients with myocardial infarction. These studies provide proof-of-concept and pave the way to an era of exciting new possibilities for anti-inflammatory therapies to treat cardiovascular diseases.

RIPK1 (receptor-interacting serine/threonine-protein kinase 1) and RIPK3 (receptor-interacting serine/threonine-protein kinase 3) belong to a family of serine-threonine kinases that execute innate immune signaling and cell stress pathways.¹⁷ Activation of TNFR1 (TNF receptor 1) recruits and assembles complex I, consisting of RIPK1, adaptor proteins (eg, TRADD [TNF receptor–associated death domain] and TRAF2 [TNF receptor–associated factor 2]), E3 ubiquitin ligases, and cellular inhibitor of apoptosis at the cytoplasmic tail of the receptor. Cell survival and death pathways are carefully orchestrated by reciprocal phosphorylation and ubiquitination of RIPK1. When RIPK1 is modified by ubiquitination, it forms a scaffold for the stabilization of IKK α /IKK β (I κ B kinase α /I κ B kinase β), degradation of I κ B α , release of NF- κ B, and activation of inflammation and prosurvival genes.¹⁸ When RIPK1 is deubiquitinated, this promotes RIPK1 activation of apoptosis and necroptosis.¹⁹ To activate necroptosis, RIPK1 interacts with and activates RIPK3, which subsequently recruits and phosphorylates the pseudokinase MLKL (mixed lineage kinase domain-like protein). MLKL oligomerizes and promotes the rupture of the plasma membrane, causing release of ATP, mitochondria, and other damage-associated molecular patterns and a cell that shares morphological features with necrosis. The balance of RIPK1 signaling in response to inflammatory challenges

is necessary to control cell survival, death, and mounting an inflammatory response.^{20,21} However, the precise ways in which RIPK1 controls these pathways are still being elucidated. We and others have previously shown that therapeutic targeting of RIPK3 phosphorylation or its genetic deletion markedly reduces macrophage necroptosis and the development of the necrotic core within the atherosclerotic plaque, promoting lesion stability in advanced atherosclerosis.^{22,23} Deletion of RIPK3 only reduced atherosclerotic lesion area after long-term Western diet feeding, but it did not protect against early atherosclerosis, suggesting that necroptosis may not contribute to lesion initiation.²³ Unlike RIPK3, the role for its upstream regulator RIPK1 in atherosclerosis has not been studied.

Here, for the first time, we investigate the role of RIPK1, a coordinator of NF- κ B inflammation and cell death, in atherosclerosis. We find that RIPK1 expression is highly expressed in early atherosclerotic lesions in humans and mice. In vitro, both basal and TNF α -stimulated NF- κ B activity and resultant inflammatory gene expression are reduced in macrophages and endothelial cells when RIPK1 is silenced. In vivo, therapeutic administration of RIPK1 antisense oligonucleotides (ASOs) markedly reduces atherosclerotic lesion size and macrophage content. Together, these findings suggest that RIPK1 drives inflammation in early atherosclerosis, and targeting RIPK1 provides a novel preventative therapeutic strategy to treat atherosclerosis.

METHODS

The data, methods, and study samples will be made available to other researchers for purposes of reproducing the results or replicating the procedures according to the American Heart Association journals' implementation of the Transparency and Openness Promotion Guidelines.

Reagents

Human LDL was purchased from Alfa Aesar and oxidized according to previous methods (Cu₂SO₄ oxidation 6 hours).²⁴ M-CSF (macrophage colony-stimulating factor) and TNF α were obtained from BioLegend. Mouse IL-1 α and IL-1 β DuoSet ELISA kits were from R&D Systems. zVAD.fmk (zVAD) and lipopolysaccharide (LPS) were purchased from BioVision and Sigma-Aldrich, respectively.

Human Atherosclerosis

All human studies were done with approval from institutional review committees and subjects gave informed consent. To determine the association between RIPK1 mRNA expression levels and other markers of interest in human carotid plaques, Pearson correlations were calculated from the microarray data set belonging to BiKE (Biobank of Karolinska Endarterectomies) (GEO [Gene Expression Omnibus] database access: GSE21545), using GraphPad Prism 6 software. The data set contains 127 plaques from patients who

underwent surgery for high-grade (>50% NASCET [North American Symptomatic Carotid Endarterectomy Trial]) carotid stenosis at the Department of Vascular Surgery, Karolinska University Hospital, Stockholm, Sweden.²⁵ The BiKE study cohort demographics, details of sample collection and processing, and transcriptomic analyses by microarrays were previously described in detail.²⁶ Human carotid endarterectomy sample data were also obtained from an independent data set (GEO access: GSE43292) from the NCBI GEO data repository,²⁷ where RIPK1 and CD68 expression values were obtained by comparing severe plaque (stage IV and V) to adjacent areas with early disease only (no macroscopic disease, stage I and II).²⁸

For immunofluorescence analysis, human coronary artery samples were obtained from the CVPath Institute Sudden Cardiac Death registry as previously described.²⁹ Comprehensive analysis of coronary artery histology was performed for each subject, and the samples were categorized as control lesions with pathological intimal thickening, early and late fibroatheromas by examining hematoxylin and eosin staining. Formalin-fixed and paraffin-embedded coronary artery blocks were sectioned at 5 mm thickness. These sections were stained with RIPK1 polyclonal antibody (No. PA5-2811, ThermoFisher, 1:100) and then with secondary goat anti-rabbit antibody (No. AA11037, ThermoFisher, 1:500).

Experimental Animals

Male and female C57Bl/6 wild-type and ApoE^{-/-} mice were purchased from Charles River or Animal Resources Center (Western Australia). RIPK1^{KD} (RIPK1^{K45A}) mice were a generous gift from Dr Peter Gough³⁰ (GlaxoSmithKline) and ApoE^{-/-}/NF- κ B transgenic mice were provided by Dr Mark Feinberg (Brigham & Women's Hospital, Boston).³¹ All animal studies were permitted by the University of Ottawa Animal Care and Use Committee in accordance with the international standards established by the Canadian Council on Animal Care or The University of Queensland Animal Ethics Committee (IMB/337/19) in Australia.

Gene Expression Analysis in Mouse Aorta

Gene expression analysis in mouse aorta from the Hybrid Mouse Diversity Panel was performed as described previously.³² In brief, the Hybrid Mouse Diversity Panel consists of \approx 100 unique inbred mouse strains that have been phenotyped extensively for cardiometabolic traits that can be correlated to gene expression data. We analyzed aortic gene expression from mice across the 100 strains fed a 1% cholesterol-enriched diet, as described previously.³³ All correlations were calculated using biweight midcorrelation (implemented in the bicor) function from the WGCNA R package), which is analogous to Pearson correlation but is more robust to outliers because the underlying calculations are median based rather than mean based and are expressed as correlation coefficient (*R*) and *P* value.

To examine gene expression in the lesser and greater curvature, *Ldlr*^{-/-} mice were fed a Western diet for 4 weeks and the ascending aorta was dissected, and cells were extracted through a DNase I and Liberase enzyme treatment as previously described.³⁴ Enzymes were then quenched and washed,

and intimal cells were gently scraped into RNA extraction buffer (MicroRNAeasy RNA isolation kit, Qiagen). Isolated RNA was reverse transcribed using High-Capacity cDNA Reverse Transcription kit (Applied Biosystems) and quantitative reverse transcription polymerase chain reaction was performed using SYBR Green I Master mix (Roche) according to the manufacturer's instructions. Gene expression was normalized to hypoxanthine-guanine phosphoribosyltransferase using the Delta-Delta Ct method.

Macrophage Isolation

Bone marrow cells were isolated from femurs of adult wild-type mice and differentiated into macrophages (bone marrow-derived macrophages) using DMEM supplemented with 10% fetal bovine serum, 1% penicillin-streptomycin, and either 20% L929 conditioned medium or 20 ng/mL M-CSF as previously described.¹⁰ To polarize macrophages to M1 or M2, cells were treated with 500 ng/mL LPS and 100 ng/mL interferon- γ , or 10 ng/mL IL-4 (interleukin 4) for 24 hours. For oxidized low-density lipoprotein (oxLDL) treatment, cells were treated with 100 μ g/mL oxLDL with or without 50 μ mol/L zvad.fmk.

Wild-type, adult mice (8 weeks old) were subjected to an intraperitoneal injection of 1 mL of 3% or 10% thioglycollate. For in vivo transfection of ASOs, 3 days after thioglycollate injection, the mice are subjected to another intraperitoneal injection of 50 mg/kg either control (CCTTCCTGAAGGTTCTCC a random nontargeting sequence) or RIPK1 (TCAGCCACTTCTGAAGCATT) ASOs from Ionis Pharmaceuticals. On day 4 after thioglycollate, peritoneal macrophages were isolated by peritoneal lavage with 2 \times 5 mL sterile phosphate-buffered saline as described.³⁵ Cells were centrifuged, resuspended in DMEM supplemented with 10% fetal bovine serum, 1% penicillin-streptomycin, and seeded at 4 \times 10⁶ cells/well in a 6-well plate, 1 \times 10⁶ cells/well in a 24-well plate, and 0.2 \times 10⁶ cells/well in a 96-well plate and incubated at 37°C for 24 hours. Cells were treated with 100 μ g/mL oxLDL, 50 ng/mL TNF α , 50 μ mol/L zvad.fmk, as described in the figure legends. For cytokine ELISAs, cells were primed with 200 ng/mL LPS and then treated with 50 μ g/mL oxLDL for 18 hours.

Endothelial Cells

Primary human umbilical vein endothelial cells (HUVECs) were isolated from human umbilical cords obtained at the Leiden University Medical Center after written informed consent and ensuring that collection and processing of the umbilical cord was performed anonymously. The umbilical vein was flushed with phosphate-buffered saline, using glass cannulas, to remove all remaining blood. Endothelial cells were detached by infusion of the vein with Trypsin/EDTA (1 \times) (Lonza, BE02-007E) solution and incubation at 37°C for 15 minutes. After incubation, the cell suspension was collected and taken up in endothelial cell growth medium (EGM2 medium, Promocell, C-22010) with 1% antibiotics. After flushing the umbilical vein once more with phosphate-buffered saline, to ensure all detached cells are collected, cells were pelleted by centrifugation at 1200 rpm for 7 minutes. The cell pellet was dissolved in fresh EGM2 medium and cells were cultured on gelatin (1%) coated surfaces. For TNF α stimulation, HUVECs

were incubated with 2 ng/mL TNF α for 24 hours, unless indicated otherwise. To achieve a knockdown of RIPK1, HUVECs were transduced with lentiviral particles encoding short hairpin RNA targeting RIPK1 (MISSION library Sigma-Aldrich, TRCN0000000705, TRCN0000000706, TRCN0000000708, TRCN0000200006) or a scrambled control short hairpin RNA (mock). Selection of transduced cells was achieved using puromycin (2 μ g/mL).

Monocyte Adhesion Assay

THP1 cells (ATCC, TIB-202) were cultured in RPMI 1640 medium (Gibco, 22409) supplemented with 10% fetal calf serum, 1% L-glutamine, 1% antibiotics (penicillin/streptomycin, Gibco, 15070063), and 25 nmol/L β -mercaptoethanol. THP1 cells were labeled with 5 μ g/mL Calcein AM (Molecular Probes Life Technologies, C3100MP) and incubated on top of a monolayer of HUVECs, pretreated with 2 ng/mL TNF α for 24 hours, for 30 minutes at 37°C. Nonadherent cells were washed away by multiple washing steps with phosphate-buffered saline after which the cells were lysed in Triton-X 0.5% for 10 minutes. Fluorescence was measured at excitation wavelength 485 nm and emission wavelength 514 nm. Each condition was performed in triplicate.

Gene Expression

Treated cells were lysed in TRIzol reagent (Invitrogen) according to the manufacturer's recommendations, and complementary DNA was synthesized using iScript Reverse Transcription kit (Bio-Rad). Quantitative polymerase chain reaction was performed in triplicate using TaqMan Gene Expression Assay and mRNA level was normalized to either β -2-microglobulin or hypoxanthine-guanine phosphoribosyltransferase. For HUVECs, total RNA was reverse transcribed using M-MLV Reverse Transcriptase Kit (Promega, M1701). Reverse transcription polymerase chain reaction analysis was conducted using SYBR Select Master Mix (Applied Biosystems, 4472908). mRNA expression was normalized to expression of GAPDH.

Western Blot

Peritoneal macrophages (1.8 \times 10⁶ per well) were lysed directly in 2 \times SDS sample buffer (Bio-Rad) and subjected to SDS-PAGE and Western blot analysis with RIPK1 antibody (1:1000, No. 610458, BD Transduction Laboratories).

Cell Viability Assays

Lactate dehydrogenase release into the medium was detected as a kinetic assay by measuring absorbance at 340 nm for 1-minute intervals for 10 minutes as previously described.¹⁰ The slope of the curve was expressed as a fold change relative to control.

NF- κ B Luciferase Assay

Adult ApoE^{-/-}/NF- κ B-reporter mice were fed a chow or Western diet (0.2% cholesterol; Harlan Teklad) for 4 weeks. These mice were then subjected to an intraperitoneal injection of thioglycollate, followed by another intraperitoneal injection of control or RIPK1 ASO for 36 hours before isolation of macrophages. The NF- κ B promoter activity was measured as

luciferase signal detected by using the Dual-Luciferase assay (Promega) according to the manufacturer's instructions. All assays were performed from either 3 (Western diet-fed) or 6 (LPS-treated) mice per group in 4 technical replicates.

Immunofluorescence of HUVECs

For immunofluorescence staining, HUVECs were cultured on μ -Slide 8 well (Ibidi, C80826), stimulated with or without 2 ng/mL TNF α for 24 hours, and fixed with 4% formaldehyde (w/v in Hank's balanced salt solution [HBSS] supplemented with calcium and magnesium [HBSS+]), Gibco) for 10 minutes. Cells were then permeabilized with 0.1% Triton X-100 and blocked with 5% BSA (wt/wt in HBSS+) for 30 minutes. The primary antibody was prepared in 0.5% BSA (w/wv in HBSS+): intercellular adhesion molecule 1 mouse anti-human antibody (Santa Cruz Biotechnology, SC-107, 1:50), NF- κ B p65 rabbit anti-human antibody (Cell Signaling Technology, 8242, 1:400). Incubation of the primary antibody was done at room temperature for 1 hour. The secondary antibody was also prepared in 0.5% BSA (goat anti-mouse IgG alexa 488, goat anti-rabbit alexa 647, Invitrogen, 1:500), together with Rhodamine Phalloidin (Invitrogen, 1:200) and Hoechst 33528 (Invitrogen, H3569, 1:2000) to stain F-actin and cell nuclei. Fluorescence images were captured by using the ImageXpress (Molecular Devices) and analyzed using ImageJ software.

Atherosclerosis Studies

Eight-week-old female and male ApoE^{-/-} mice (9–12/group) were fed an adjusted calories Western diet (21% fat, 0.2% cholesterol; Harlan Teklad) for 8 weeks and were randomly assigned to simultaneously receive weekly subcutaneous injections of 100 mg/kg control ASO (CCTTCCCTGAAGTCTCTCC) or RIPK1 ASO (TCAGCCACTTCTGAAGCATT) or for indicated experiments, RIPK1 ASO-B (CTCCATGACTCCATACCA). After 8 weeks, mice were euthanized; perfused with saline; the aortic root, ascending and descending aorta, and liver were collected as previously described.^{10,35,36} In brief, aortic sinuses were embedded in optimum cutting temperature compound medium, frozen, sectioned (10 μ m), and stained with hematoxylin and eosin for quantifications, where a minimum of 8 to 10 sections per animal were measured across the length of the entire aortic root. For en face aortic lesion quantifications, dissected aortas (down to the femoral bifurcation) were sliced ventrally and imaged; the lesion area was quantified by a nonblinded user using ImageJ. To visualize macrophages, smooth muscle cells (SMCs), IL-1 α immunofluorescence was performed using Mac-2 antibody (Cedarlane, CL8942AP) followed by Alexa488-conjugated secondary antibody, SMC α (monoclonal antibody conjugated to alkaline phosphatase, Sigma, A5691) or IL-1 α (Abcam ab7632) followed by Alexa594-conjugated secondary antibody. Sections were imaged using the Leica ScanScope. Fluorescent positive areas were quantified using ImageJ. Serum cytokines were analyzed using Bioplex Pro Mouse Cytokine Assay (no. M60009RDPD; Bio-Rad) according to the manufacturer's instructions.

Statistical Analysis

Data shown are either a representative mean \pm SD experiment of at least 3 experiments or mean \pm SEM of experiments

performed in triplicate, as indicated in the corresponding figure legend. For comparison between 2 groups, Student *t* tests (unpaired) were used, unless otherwise stated, and *P*-values are indicated in the figure legends. For comparison between groups, 1- or 2-way ANOVA (*P* \leq 0.05) with multiple comparisons tests was performed using Graphpad Prism.

RESULTS

RIPK1 Expression Is Increased in Early-Stage Atherosclerotic Lesions

To begin to understand how RIPK1 might be contributing to lesion development, we examined its expression in lesions with different degrees of atherosclerotic disease burden. In human coronary arteries with disease classified as pathological intimal thickening or in those with larger early fibroatheromas, RIPK1 protein was detected within the intimal space (Figure 1A; red). Double immunostaining in these arteries indicates that RIPK1 is expressed both in macrophages (marked by CD68) and endothelial cells (marked by vWF; Figure 1B). In endarterectomy samples from individuals with carotid atherosclerosis, the mRNA expression of RIPK1 correlated strongly with the expression of genes in the NF- κ B pathway *IKKA*, *IKKB*, *NFKB1*, and the downstream effector *IL-1A* (Figure 1C, all *P* $<$ 0.0001). In another gene expression data set from human carotid endarterectomies (GEO data set GSE43292), we find that the expression of RIPK1 on a per macrophage basis (ie, per copy of *CD68* gene expression) is higher in lesions with early-stage disease (stages I and II) than in adjacent regions with more severe plaque (stages IV and V) (Figure 1D). To further evaluate *Ripk1* expression in mouse atherosclerosis, we compared gene expression across 100 strains of outbred mice from the Hybrid Mouse Diversity Panel and find that expression of *Ripk1* in the aorta strongly correlates with expression of *Ikbkb*, an activator of the NF- κ B pathway (Figure 1E). In mice with early-stage atherosclerotic lesions (*Ldlr*^{-/-} mice fed a high-fat diet for 4 weeks³⁴), we find that gene expression of both *Ripk1* and markers of inflammation (*Tnfa*, *Ccl2*, *Il1b*) are higher in the athero-susceptible, lesser curvature of the aorta relative to the athero-resistant greater curvature aortic region (Figure 1F). Together, these data demonstrate that RIPK1 is highly expressed in early-stage atherosclerotic lesions in both humans and mice and correlates with indices of inflammation in the plaque.

Loss of *Ripk1* Reduces Macrophage Inflammation In Vitro and NF- κ B Activation In Vivo

We next set out to assess the expression profile of RIPK1 in inflammatory macrophages in vitro. We measured

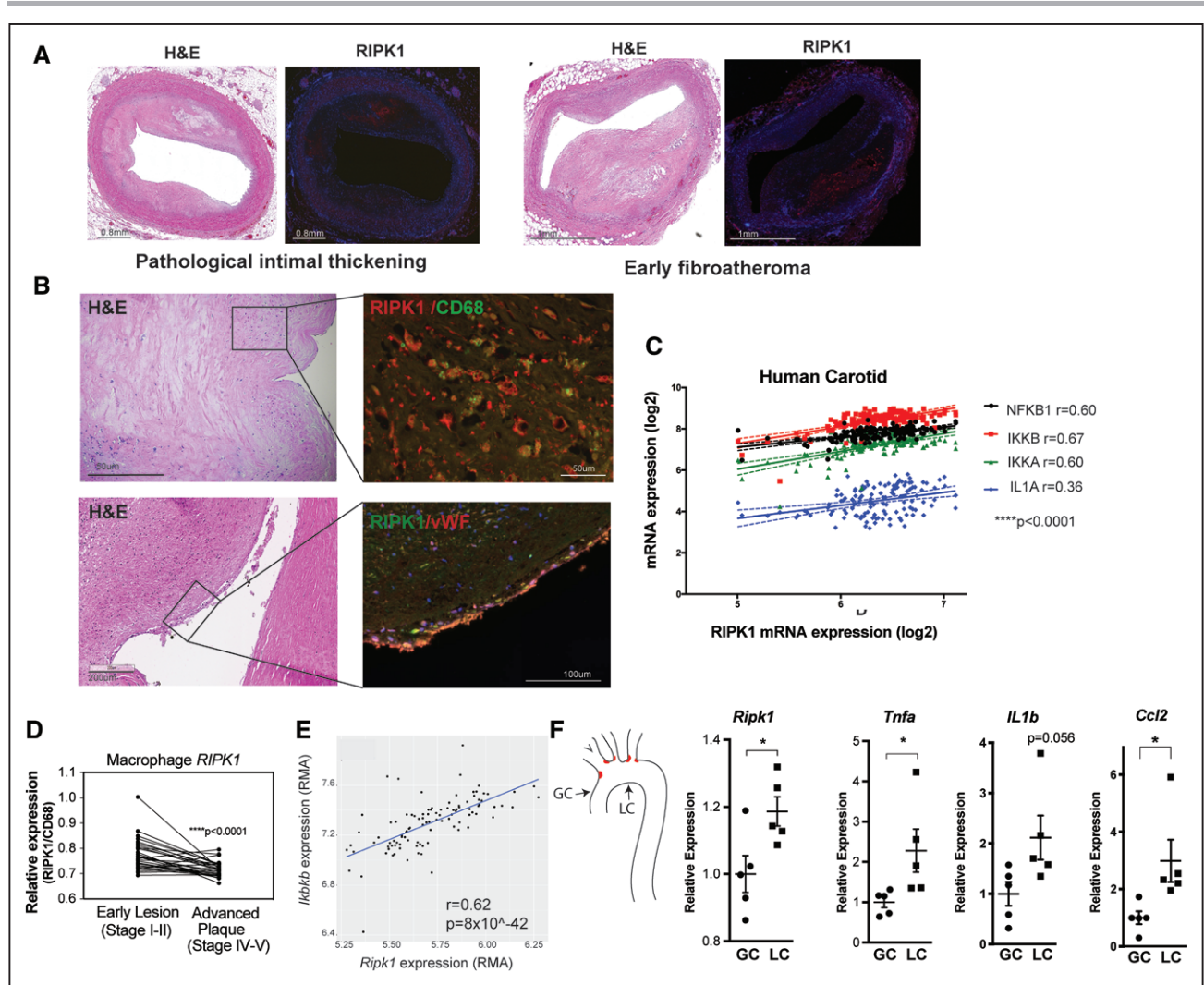


Figure 1. RIPK1 is expressed in human and mouse atherosclerotic lesions. **A** and **B**, Human coronary arteries with atherosclerotic lesions classified as either pathological intimal thickening or early fibroatheroma. H&E staining and RIPK1 staining (red) indicate that RIPK1 is expressed in both stages of lesion development (**A**) in both CD68+ (macrophages) and vWF+ cells (endothelial cells) (**B**). **C**, Correlations of the RIPK1 transcript with expression of *NFKB1*, *IKKB*, *IKKA*, and *IL1A* in human carotid arterectomies (n=127). *****P*<0.0001 by Pearson correlation. **D**, Analysis of *RIPK1* gene expression data from human carotid artery lesions classified as early (stage I–III) or advanced (stage IV and V) from Gene Expression Omnibus data set GSE43292 normalized to the expression of CD68. *****P*<0.0001 by paired *t* test. **E**, *Ripk1* mRNA expression in the aorta of mice from the Hybrid Mouse Diversity Panel (100 inbred strains of mice) and the correlation with *Ikbkb* mRNA in the aorta. Correlation coefficient (*r*) and *P* value were calculated as described in the Methods. **F**, Mouse *Ripk1*, *Tnfa*, *Il1b*, and *Ccl2* gene expression in athero-prone (LC) and athero-protective (GC) regions of atherosclerotic lesions isolated from *Ldlr*^{-/-} mice fed a high-fat diet for 4 weeks. **P*≤0.05, Student *t* test. GC indicates greater curvature; H&E, hematoxylin and eosin; LC, lesser curvature; RIPK1, receptor-interacting serine/threonine-protein kinase 1; RMA, robust multi-array average; and vWF, von Willebrand factor.

Ripk1 gene expression in bone marrow–derived macrophages polarized to either a proinflammatory M1 or anti-inflammatory M2 macrophages, and we observed a 3.2-fold increase in *Ripk1* gene expression in M1 macrophages relative to nontreated M0-macrophages, whereas *Ripk1* levels in M2 macrophages were unchanged (Figure 2A). We had previously shown that oxLDL induces the expression of necroptotic genes, *Ripk3* and *Mlkl*. Here, we similarly find that oxLDL and oxLDL+zVAD treatment of bone marrow–derived macrophages resulted in a 1.4- and 1.8-fold increase in *Ripk1* gene expression, respectively (Figure 2B).

Using ASOs to knockdown expression of *Ripk1*, we evaluated the activation of inflammation in vivo

in thioglycollate-elicited macrophages in the peritoneal cavity. Intraperitoneal injection of RIPK1 antisense decreased both *Ripk1* gene and protein expression relative to control, as expected (Figure 2C). In macrophages treated with RIPK1 antisense, we also found a reduction in baseline expression of inflammatory transcripts *Nfkb1* and *Tnfa* (67.46%±21.55% and 58.85%±24.75%) and a decrease in inflammasome-related genes *Casp1*, *Nlrp3*, *Il1a*, and *Il1b* (55.45%±31.03%, 61.92%±27.87%, 44.07%±7.52%, 55.22%±6.99%, respectively), as well (Figure 2D). To investigate the role of RIPK1 in driving TNFα- or oxLDL-induced inflammation, we isolated peritoneal macrophages after RIPK1 silencing

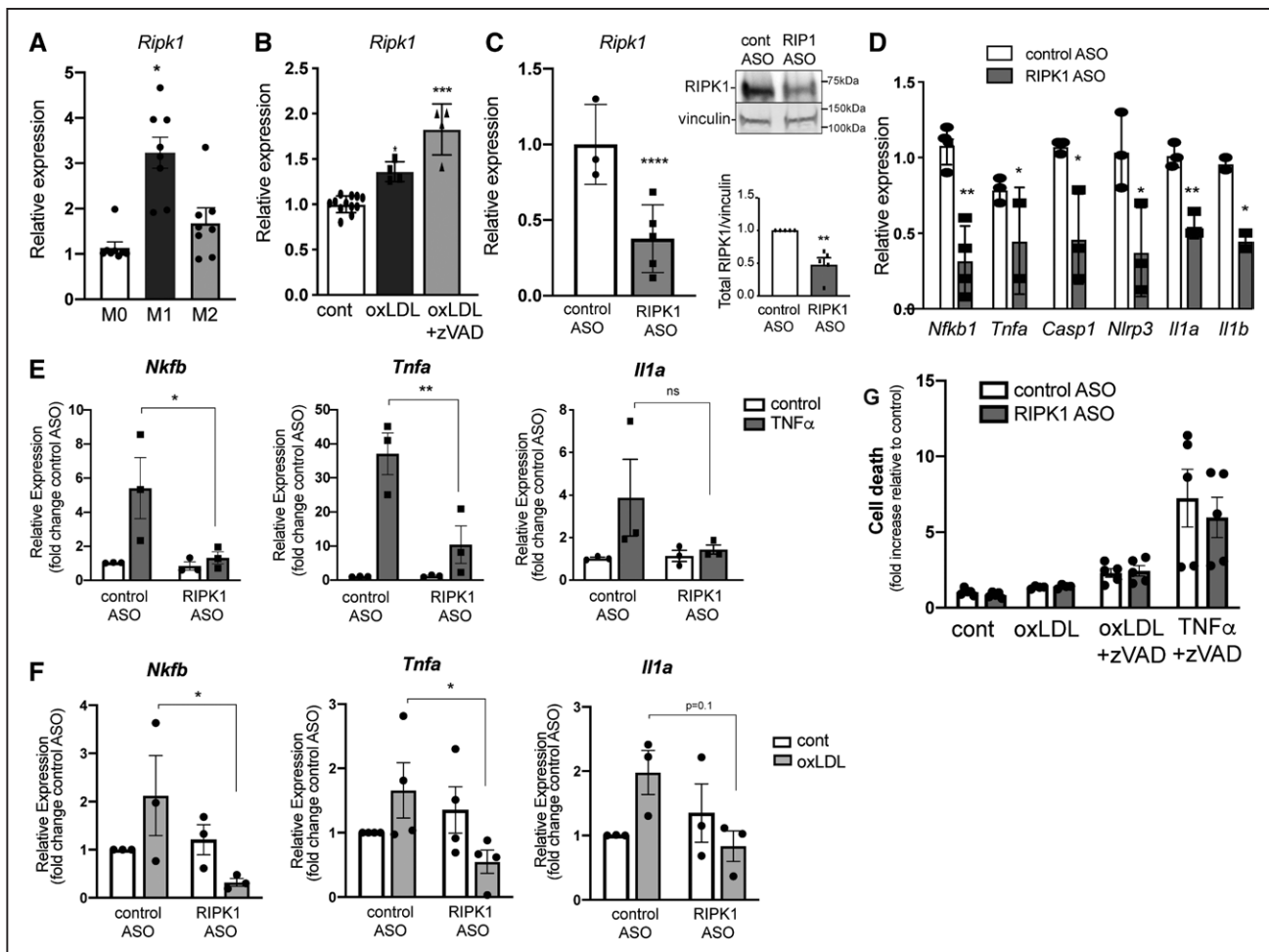


Figure 2. *Ripk1* expression is induced in inflammatory macrophages and knockdown of *Ripk1* reduces inflammatory gene activation.

A, *Ripk1* gene expression in bone marrow–derived macrophages polarized to either a proinflammatory M1 (lipopolysaccharide and interferon- γ treated) or anti-inflammatory M2 (IL-4 treated) macrophages. **B**, Treatment of bone marrow–derived macrophages with 100 $\mu\text{g}/\text{mL}$ oxLDL, with or without 50 $\mu\text{mol}/\text{L}$ zVAD before RNA isolation and analysis of *Ripk1* gene expression relative to housekeeping genes. For **A** and **B**, $*P < 0.01$ and $***P < 0.001$ by 1-way ANOVA and Tukey multiple comparisons test. **C** and **D**, Intraperitoneal injection of 50 mg/kg control ASO or RIPK1 ASO before peritoneal macrophage isolation and gene expression analysis of *Ripk1* (**C**) and inflammatory genes *Nfkb1*, *Tnfa*, *Casp1*, *Nlrp3*, *Il1a*, and *Il1b* (**D**). **C** and **D**, $*P \leq 0.05$, $****P < 0.0001$ by unpaired Student *t* test. **E** and **F**, Peritoneal macrophages transfected with control ASO or RIPK1 ASO and treated with 50 ng/mL TNF α or 100 $\mu\text{g}/\text{mL}$ oxLDL before gene expression analysis of *Nfkb*, *Il1a*, and *Tnfa*. **G**, Cell viability of peritoneal macrophages transfected with control ASO or RIPK1 ASO and treated with oxLDL, oxLDL+zVAD, TNF α +zVAD, lipopolysaccharide+zVAD. For **E** through **G**, $*P < 0.05$, $**P < 0.01$, and $***P < 0.001$ by 2-way ANOVA and Sidak multiple comparisons test. ASO indicates antisense oligonucleotide; cont, control; ns, not significant; oxLDL, oxidized low-density lipoprotein; RIPK1, receptor-interacting serine/threonine-protein kinase 1; TNF α , tumor necrosis factor α ; and zVAD, pan-caspase inhibitor z-Vad-fmk.

and treated the cells with TNF α or oxLDL before analyzing inflammatory gene expression. The TNF α - and oxLDL-stimulated expression of *Nfkb1*, *Il1a*, and *Tnfa* was reduced in peritoneal macrophages transfected with RIPK1 antisense (Figure 2E and 2F). We and others have shown that atherogenic ligands induce RIPK3-dependent necroptosis,^{10,23,37} and inactivation of RIPK1 kinase activity has been shown previously to reduce necroptotic cell death.^{30,38} We therefore tested whether reducing RIPK1 gene expression also affected the activation of necroptosis. We observed that knocking down RIPK1 did not affect necroptotic ligand (oxLDL, oxLDL+zVAD, TNF α +zVAD, LPS+zVAD)-induced cell death in peritoneal macrophages unlike what is observed in peritoneal macrophages from RIPK1 kinase-dead (RIPK1^{K45A}) mice (Figure 2G and Figure IA

and IB in the Data Supplement). Together, these data suggest that knocking down RIPK1 impairs the ability of macrophages to promote NF- κ B-mediated inflammation while maintaining their capacity for necroptotic cell death.

To test whether RIPK1 directly targets NF- κ B activity in atherogenic macrophages, we used transgenic *ApoE*^{-/-} mice expressing the NF- κ B promoter upstream of a green fluorescent protein/luciferase fusion reporter gene.^{31,39} Macrophages were elicited into the peritoneal cavity of *ApoE*^{-/-}/NF- κ B reporter mice, injected with control or RIPK1 antisense, followed by a single LPS injection to induce an inflammatory response. As expected, LPS treatment significantly increased NF- κ B promoter activity in *in vivo* macrophages (9-fold), and this was inhibited in RIPK1-silenced macrophages

(Figure 3A). We were then interested in whether atherogenic inflammatory activation of NF- κ B was also inhibited by RIPK1 knockdown; therefore, we fed *ApoE*^{-/-}/NF- κ B reporter mice a Western diet (0.2% cholesterol) for 4 weeks to induce hypercholesterolemia and foam cell formation in peritoneal macrophages before delivery of control or RIPK1 ASOs. Peritoneal macrophages isolated from Western diet-fed mice had a 1.7-fold increase in NF- κ B activity in comparison with chow diet-fed mice (Figure 3B). RIPK1 antisense-transfected *in vivo* peritoneal macrophages isolated from both chow-fed and Western diet-fed mice had a marked reduction in NF- κ B luciferase activity (Figure 3B), suggesting that both basal inflammatory and diet-induced inflammatory responses were attenuated by RIPK1 knockdown. Recent studies have shown that NF- κ B activation induces gene regulation that drives NLRP3 inflammasome-dependent IL-1 β and -independent IL-1 α secretion from macrophages.⁴ To investigate the role of RIPK1 in regulating macrophage IL-1 secretion, peritoneal macrophages transfected with control or RIPK1 antisense were primed with either LPS or TNF α before stimulation with oxLDL. In comparison with control cells, RIPK1 silencing in macrophages led to a reduction in secreted IL-1 α in both LPS- and TNF α -primed macrophages (by

\approx 40% and 56%, respectively; Figure 3C, Figure IIA in the Data Supplement). There was also decreased IL-1 β secretion in macrophages with RIPK1 antisense in LPS+oxLDL-stimulated cells (Figure 3D). IL-1 β was not detected in TNF α +oxLDL-treated supernatants (data not shown). Together, these data suggest that RIPK1 expression downstream of atherogenic and proinflammatory stimuli drives NF- κ B-dependent proinflammatory IL-1 α and IL-1 β secretion from inflammatory macrophages.

Knockdown of Endothelial RIPK1 Ameliorates TNF α -Induced Inflammation

NF- κ B activation in endothelial cells (ECs) is critical for the initiation of the inflammatory response and induces the expression of adhesion molecules and inflammatory cytokines, among others. Because we observed a significant downregulation of NF- κ B on reduction of RIPK1 in macrophages, we sought to examine the impact of *RIPK1* silencing on the endothelial inflammatory response. Treatment of HUVECs with TNF α for 24 hours induced the expression of *IL1B* in control ECs, but this response was reduced \approx 85% when *RIPK1* was silenced (Figure 4A). A similar response was observed for E-selectin

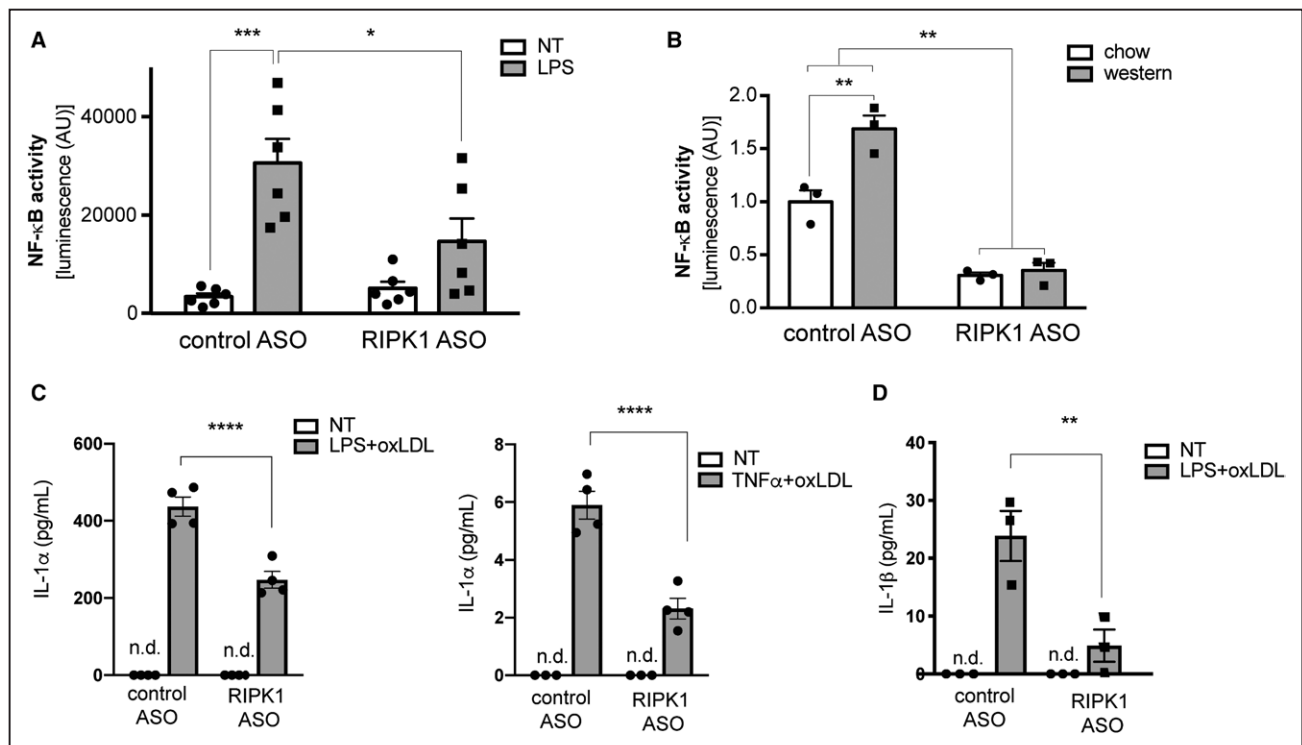


Figure 3. RIPK1 ASO markedly inhibits NF- κ B activation in response to inflammatory stimuli *in vivo*.

A, Peritoneal macrophages were elicited in male and female *ApoE* (apolipoprotein E)-NF- κ B reporter mice ($n=6$ /group) with intraperitoneal injection of thioglycollate and, at day 3, the mice were administered 50 mg/kg control or RIPK1 ASO intraperitoneal injection. On day 5, the mice were subjected to intraperitoneal injection of 200 ng of LPS for 1.5 hours before the isolation of macrophages. **B**, Eight-week-old male mice ($n=3$ /group) were subjected to a Western diet for 4 weeks before eliciting peritoneal macrophages and administration of RIPK1 ASOs as described in **A**. **C** and **D**, Wild-type peritoneal macrophages treated with 50 mg/kg control or RIPK1 ASO were primed with 200 ng/mL LPS or 50 ng/mL TNF α and treated with 50 μ g/mL oxLDL for 18 hours *in vitro*. Secreted IL-1 α (**C**) and IL-1 β (**D**) were measured using ELISA. * $P<0.05$, ** $P<0.01$, and **** $P<0.001$ by 2-way ANOVA and Sidak multiple comparisons test. ASO indicates antisense oligonucleotide; IL, interleukin; LPS, lipopolysaccharide; n.d., not detected; NF- κ B, nuclear factor κ -light-chain-enhancer of activated B cells; NT, no treatment; oxLDL, oxidized low-density lipoprotein; RIPK1, receptor-interacting serine/threonine-protein kinase 1; and TNF α , tumor necrosis factor α .

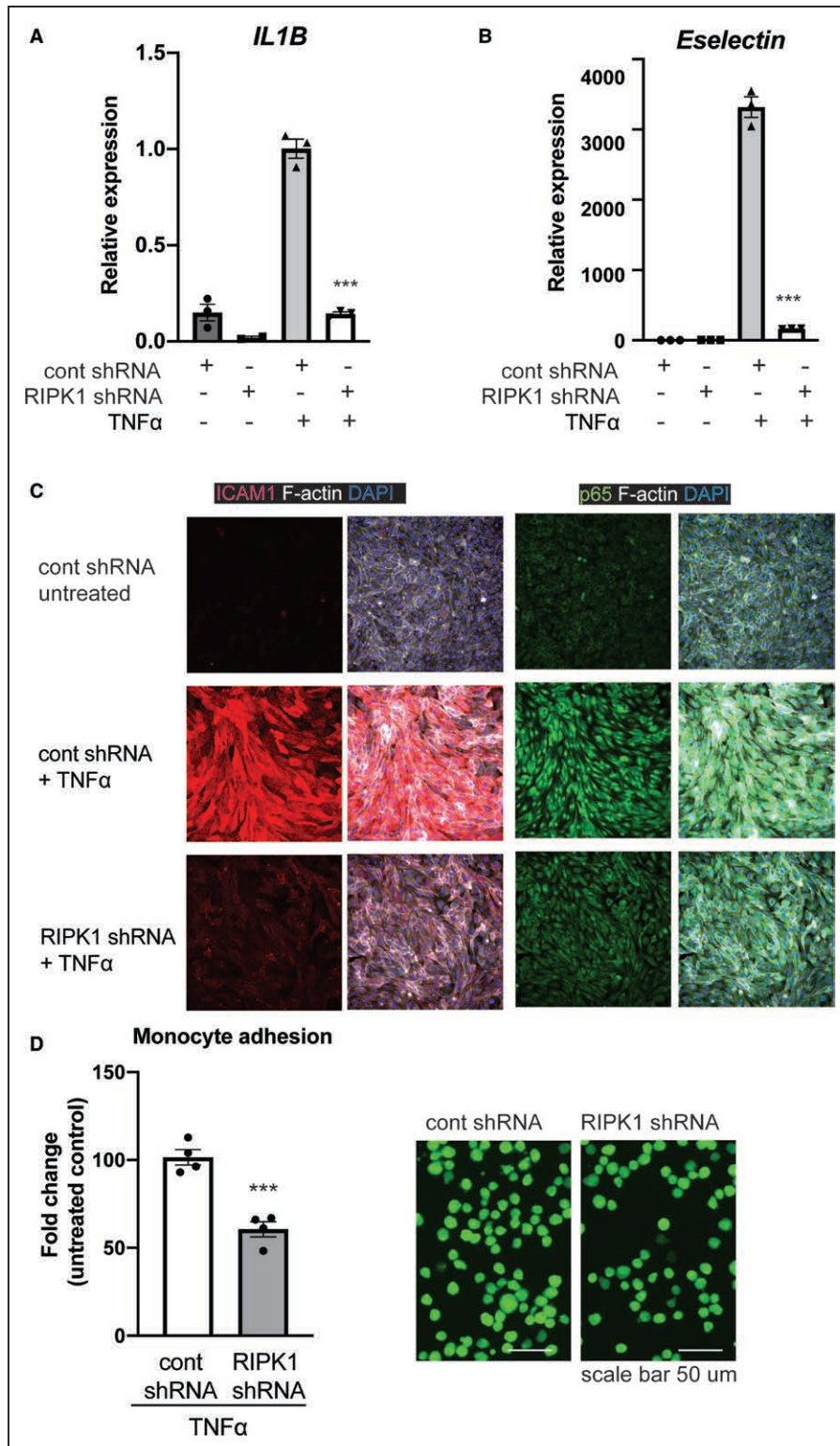


Figure 4. RIPK1 knockdown in endothelial cells reduces inflammatory gene expression and monocyte adhesion.

A through **C**, Human umbilical vein endothelial cells were transduced with lentiviral shRNA against RIPK1 (or mock control) and treated with TNF α for 24 hours before gene expression analysis (**A** and **B**) and immunofluorescence of ICAM-1 (red), p65 NF- κ B subunit (green), F-actin (white), and DAPI (blue) (**C**); n=3 per treatment, experiments performed in triplicate; ***P<0.001 versus cont shRNA through 1-way ANOVA with the Tukey multiple comparisons test. **D**, THP-1 monocytes were labeled with calcein fluorescent dye (green) and incubated on top of a monolayer of human umbilical vein endothelial cells (transduced and treated TNF α for 24 hours as mentioned) for 30 minutes at 37°C. Cells were washed extensively before visualization by microscopy and quantification by plate reader. ***P<0.001 versus cont shRNA by the Student *t* test. Cont indicates control; DAPI, 4',6-diamidino-2-phenylindole; ICAM-1, intercellular adhesion molecule 1; NF- κ B, nuclear factor κ -light-chain-enhancer of activated B cells; RIPK1, receptor-interacting serine/threonine-protein kinase 1; shRNA, short hairpin RNA; and TNF α , tumor necrosis factor α .

(SELE), where *RIPK1* knockdown reduced TNF α -induced E-selectin expression by \approx 95% (Figure 4B). Both the expression of intercellular adhesion molecule 1 and the nuclear translocation of the p65 subunit of NF- κ B were induced on TNF α treatment, and *RIPK1* knockdown blunted these responses (Figure 4C). To determine if knocking down *RIPK1* functionally altered the EC inflammatory phenotype, monocytes were incubated with ECs after stimulation with TNF α . In comparison with controls, silencing of *RIPK1* led to a decrease in monocyte adhesion to the endothelial monolayer (Figure 4D). Because complete loss of RIPK1 can lead to spontaneous cell death, we tested whether ECs with RIPK1 knockdown were more susceptible to cell death in response to TNF α . We saw no difference in cell death between control and RIPK1-silenced cells (Figure IIB in the Data Supplement). Together, the data suggest that, in addition to macrophages, RIPK1 plays a role in the activation of NF- κ B in response to inflammatory stimuli in vascular ECs.

Therapeutic Knockdown of RIPK1 Protects Against Early Atherosclerosis

Given our observation that RIPK1 expression is expressed in early lesions in both humans and mice and that RIPK1 promotes NF- κ B inflammation in response to atherogenic and inflammatory ligands in vitro, we postulated that RIPK1 inhibition during lesion initiation would reduce atherosclerotic lesion size. To test this, we administered a control or RIPK1 ASO to male and female *Apoe* $^{-/-}$ mice fed a Western diet for 8 weeks (Figure 4). Using antibodies that recognize the 2'-fluoromethoxyethyl modification on the oligonucleotides, we confirmed that ASOs were delivered to the atherosclerotic lesions and demonstrated RIPK1 knockdown in both the intimal lesion and endothelial layer (Figure IIIA in the Data Supplement). Assessment of the en face lesion area in ascending and descending aorta revealed that RIPK1 ASO significantly reduced lesion development in comparison with control ASO-treated mice (58.8% in comparison with control ASO-treated mice (Figure 5A). Furthermore, examination of aortic root lesions demonstrated that RIPK1 ASO-treated mice had a 47% reduction in lesion area in comparison with control ASO (Figure 5B). Using a second ASO directed against RIPK1 with a unique sequence (RIPK1 ASO-B), we also observed significant changes in aortic en face and sinus lesion area (Figure IIIB and IIIC in the Data Supplement). There was no difference in the en face aortic and aortic sinus lesion area between untreated (no treatment) and control ASO-treated mice (Figure IIID in the Data Supplement). There was no significant difference in total plasma cholesterol and body weight (Figure IVA and IVB in the Data Supplement). In addition, the administration of these ASOs in vivo was not toxic as reflected by the lack of differences in circulating liver enzymes, ALT (alanine aminotransferase) and

AST (aspartate aminotransferase), between no treatment, control ASO-treated, and RIPK1 ASO-treated mice (Figure IVC in the Data Supplement), and we observed a significant decrease in *Nfkb1* expression in the livers of RIPK1 ASO-treated mice (Figure 5C). To evaluate the systemic inflammatory profile of these mice, we measured the levels of circulating cytokines in the serum, and find a reduction in the proinflammatory cytokines, IL-1 α , IL-3, IL-5, IL-6, IL-12(p70), IL-17A, eotaxin, and GM-CSF (Figure 5D), whereas other proinflammatory cytokines, including IL-1 β and TNF α , remained unchanged (Figure IVD in the Data Supplement). We assessed lesion composition by immunostaining markers of macrophages (Mac-2) and SMCs (α -smooth muscle actin) within aortic sinus lesions. Consistent with a reduction in atherosclerotic progression, we detected a reduction in macrophage area by 36.92% (RIPK1 ASO, $P < 0.01$) and SMC area by 66.5% ($P < 0.001$; Figure 5E). Last, we observed a reduction in IL-1 α staining in aortic root lesions of mice administered RIPK1-ASO (Figure 5F), which is consistent with the decreased inflammation observed in these mice. Together, these data demonstrate that therapeutic silencing of RIPK1 during atherosclerotic progression induced by a Western diet is dramatically reduced by directly inhibiting NF- κ B inflammatory signaling and the secretion of proinflammatory cytokines in the serum.

DISCUSSION

In this study, we find that RIPK1 gene expression is high in early-stage atherosclerotic lesions in mice and humans and is upregulated in proinflammatory macrophages in vitro. In vitro and in vivo, knockdown of RIPK1 in macrophages and ECs reduces inflammatory gene expression in TNF α -stimulated conditions and inhibits NF- κ B activity. In macrophages, loss of RIPK1 reduces the secretion of proinflammatory cytokines, IL-1 α and IL-1 β . In the *Apoe* $^{-/-}$ mouse model of atherosclerosis, which develops large foam cell-rich inflammatory lesions with high-cholesterol diet feeding, systemic RIPK1 knockdown markedly reduces atherosclerotic lesions, with no effect on plasma cholesterol or body weight. Furthermore, both liver inflammatory gene expression and circulating serum inflammatory cytokines are also reduced in RIPK1 ASO-treated mice. Together, our study places RIPK1 at the center of inflammatory signaling during atherosclerosis development (Figure 6).

RIPK1 sits downstream of inflammatory receptors in a complex that coordinates cell survival, cell death, and activation of NF- κ B. If the TNFR1 is engaged by TNF α , a membrane-bound complex forms, promoting the modification of RIPK1 by linear K63-ubiquitination, allowing the recruitment of TAK1 (transforming growth factor- β -activated kinase 1) and stabilization of IKK α /IKK β , degradation of I κ B α , and the release and activation of MAPK (mitogen-activated protein kinase) and NF- κ B.¹⁸

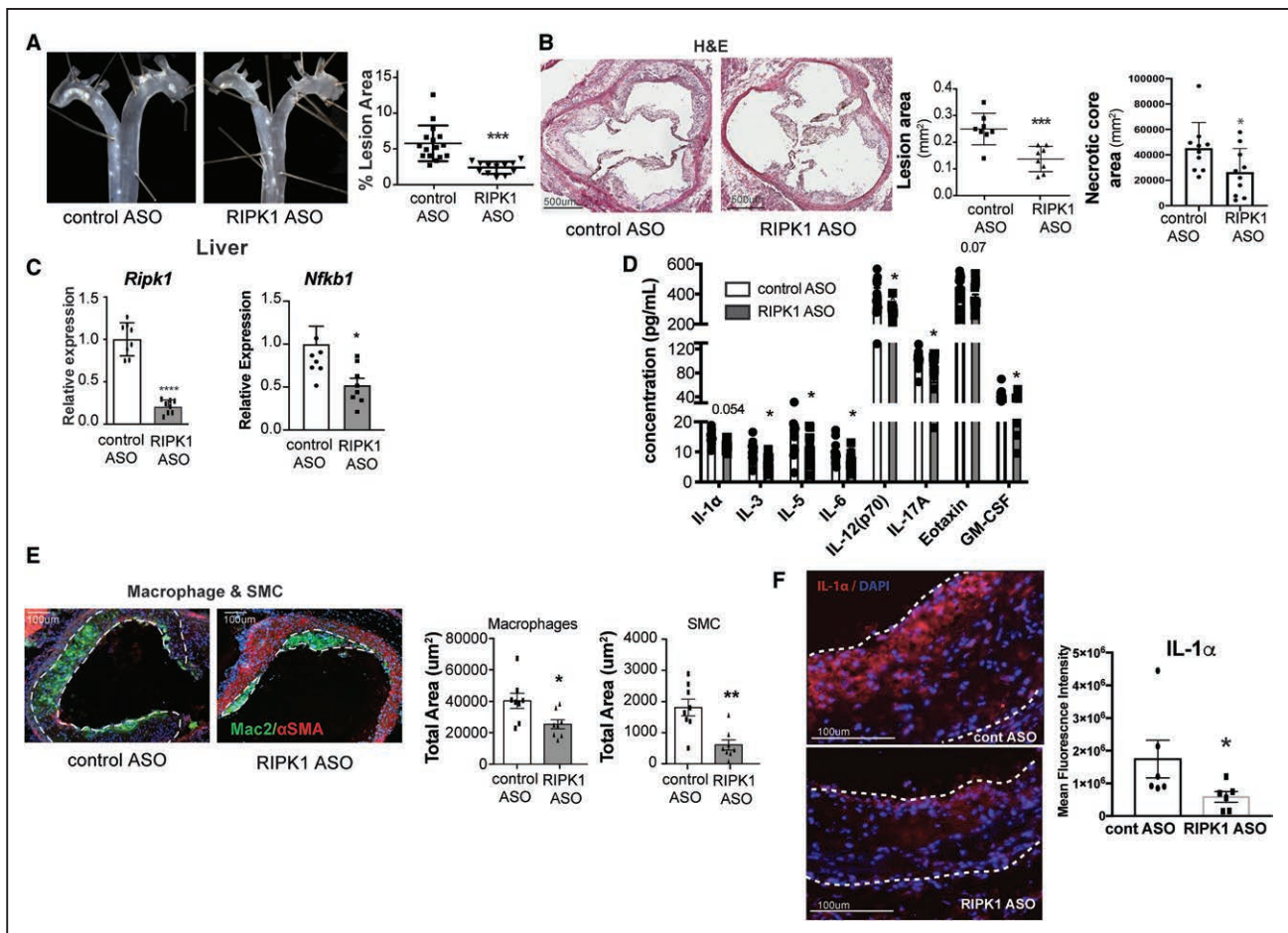


Figure 5. RIPK1 ASO reduces atherosclerotic lesion development in *ApoE*^{-/-} mice.

ApoE^{-/-} mice were fed a Western diet for 8 weeks and simultaneously treated with control ASO or RIPK1 ASO. **A** and **B**, Quantification of atherosclerotic lesion area. En face lesion area, as a percentage of total area of the aorta, in the aortic arch and descending aorta (**A**) and aortic sinus lesion area across the entire aortic root from H&E-stained sections (**B**); n=9 to 12 mice per group, **P*≤0.05, Student *t* test. **C**, Gene expression of *Ripk1* and *Nfkb1* in the liver of treated mice. **D**, Circulating cytokine levels in the plasma of cont ASO- and RIPK1 ASO-treated mice as determined by the Bioplex Mouse Cytokine Array at the end of the 8-week study; n=9 to 12 mice per treatment group. **P*≤0.05, Student *t* test. **E**, Macrophage (Mac2, green) and SMC (α -smooth muscle actin [α SMA], red) area was quantified in aortic sinus sections from cont ASO- and RIPK1 ASO-treated mice; n=9 to 12 mice per group, **P*≤0.05, Student *t* test. **F**, Immunofluorescent staining for IL-1 α in lesions from cont ASO- and RIPK1 ASO-treated mice; n=6 mice per group, **P*≤0.05, Mann-Whitney *U* test. ASO indicates antisense oligonucleotide; cont, control; DAPI, 4',6'-diamidino-2-phenylindole; GM-CSF, granulocyte-macrophage colony-stimulating factor; H&E, hematoxylin and eosin; IL, interleukin; RIPK1, receptor-interacting serine/threonine-protein kinase 1; and SMC, smooth muscle cell.

Prosurvival factors, such as MK2, that are produced by activation of MAPK and NF- κ B offset the death receptor signaling through TNFR1 largely because of inactivating the phosphorylation activity of RIPK1, thereby preventing its engagement of the apoptosis and necroptosis pathways.⁴⁰⁻⁴² The germline deletion of RIPK1 results in early postnatal lethality, which has hampered the ability to study its role in animal models of advanced or chronic disease. Cell-specific deletion of RIPK1 using Cre recombinase and floxed *Ripk1* alleles has revealed that the complete absence of RIPK1 results in cell death of hematopoietic and progenitor cells, and the intestinal epithelium and keratinocytes, as well.⁴³⁻⁴⁶ Humans with mutations in RIPK1 have severe inflammatory disorders attributable to the hyperactivation of RIPK3 and necroptosis.⁴⁷⁻⁴⁹ Although the full spectrum of RIPK1 functions under different conditions is still unclear, it appears as though RIPK1 acts as a scaffold that, during normal development and

at steady state, restricts the inappropriate activation of RIPK3 and inflammatory cell death and enables survival, MAPK and NF- κ B signaling. It is surprising that knocking down RIPK1 does not promote spontaneous cell death, nor does it impact the ability of macrophages to undergo necroptosis in response to atherogenic or necroptotic ligands. This implies that, when minimal levels of RIPK1 are maintained, RIPK1 expression favors the activation of the NF- κ B pathway in response to atherogenic ligands. This is similar to what is observed using short hairpin RNA to RIPK1 in breast cancer cells, where knockdown of RIPK1 can promote autophagy and cell survival under nutrient-depleted conditions, whereas the complete absence of RIPK1 gene sensitizes cells to cell death.^{50,51} Thus, under chronic atherogenic proinflammatory conditions, RIPK1 expression can be reduced to abrogate excessive activation of NF- κ B, while maintained at sufficient levels to prevent excessive cell death and further tissue inflammation.

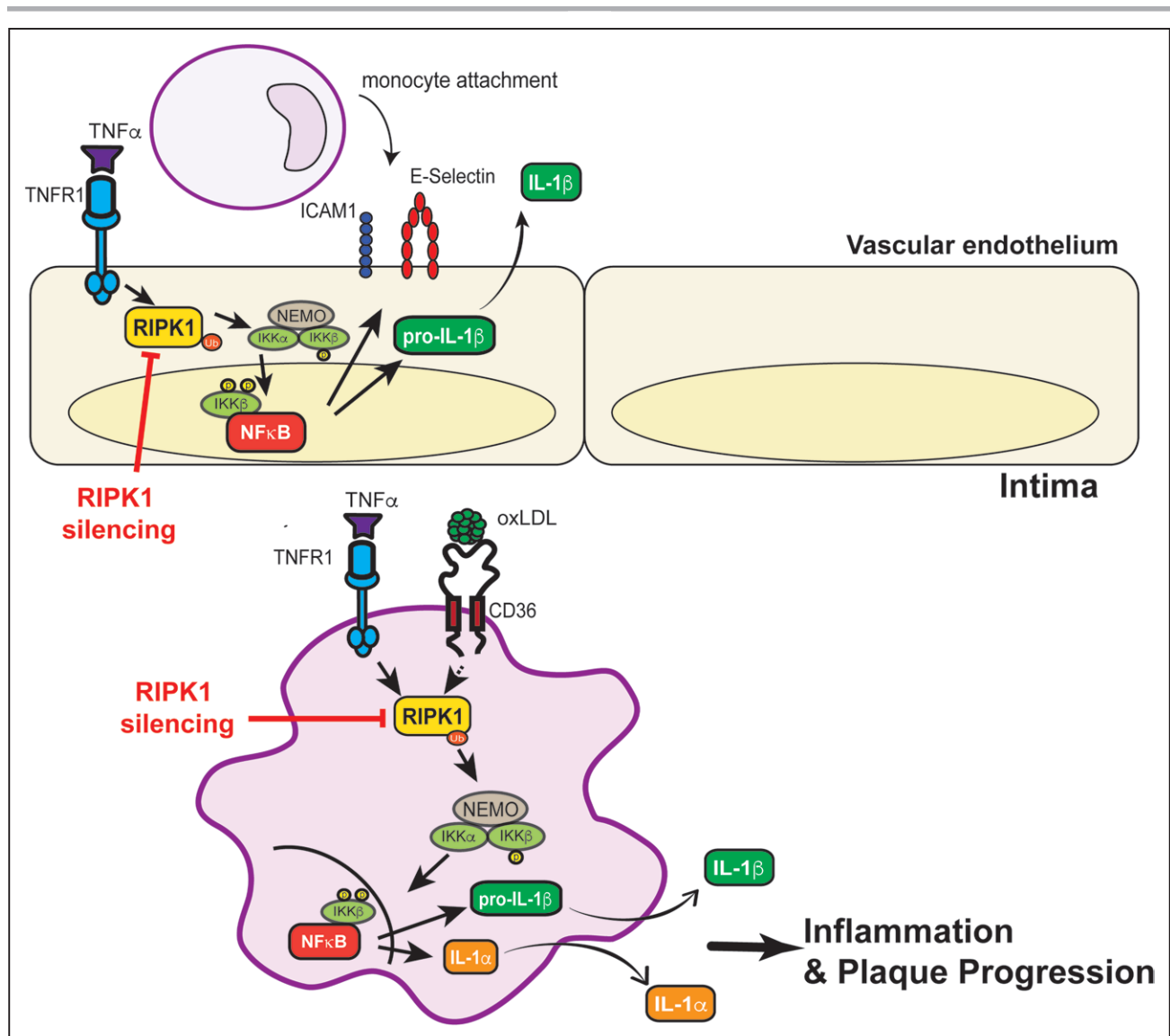


Figure 6. RIPK1 drives NF- κ B–dependent activation and cytokine secretion from within atherosclerotic lesions.

In early atherosclerosis, inflammatory stimuli such as TNF α or oxLDL stimulate RIPK1 gene expression. In vascular endothelial cells, activation through TNF α induces adhesion proteins ICAM and E-selectin, which recruits monocytes into the vascular intima. Loss of RIPK1 reduces NF- κ B activation, expression of cytokines and adhesion molecules, to reduce monocyte recruitment. In lesional macrophages, loss of RIPK1 reduces NF- κ B signaling and IL-1 α and IL-1 β production and secretion. Together, reduced RIPK1 results in reduced atherosclerotic lesion progression. ICAM-1 indicates intercellular adhesion molecule 1; IL, interleukin; NEMO, NF-kappa-B essential modulator; NF- κ B, nuclear factor κ -light-chain-enhancer of activated B cells; oxLDL, oxidized low-density lipoprotein; RIPK1, receptor-interacting serine/threonine-protein kinase 1; TNFR1, tumor necrosis factor receptor 1; and TNF α , tumor necrosis factor α .

The importance of RIPK3-mediated necroptosis in the atherosclerotic plaque has recently been elucidated, where genetic deletion of *Ripk3* reduced advanced atherosclerotic lesions and necrotic core area in both *Apoe*^{-/-} and *Ldlr*^{-/-} mice.²³ In the same way, inhibition of RIPK1-mediated necroptosis by the pharmacological inhibitor Necrostatin-1s reduced lesion complexity and necrotic core area in *Apoe*^{-/-} mice with established atherosclerosis.¹⁰ Together, these data implicate RIPK3-mediated necroptosis in necrotic core formation in advanced, established atherosclerosis. This is in contrast to the role of RIPK2, a related but distinct RIP kinase involved in host defense,^{52–54} where *Ripk2* deletion exacerbates atherosclerotic lesion development.⁵² In contrast to the other

members of the RIP kinase family, the role for RIPK1 in initiating atherosclerosis was unknown. In this study, we find robust RIPK1 gene expression within early atherosclerotic lesions in both mice and humans, where it correlates strongly with other metrics of inflammation, namely IKK and TNF α . In other words, lesional RIPK1 expression is high when inflammation is most active in promoting lesion formation. This is distinct from what is observed for phosphorylated MLKL, an effector of necroptotic cell death, that we found was uniquely expressed in large, advanced atherosclerotic plaques in humans and virtually absent in smaller, less complex lesions.¹⁰ Others have shown that TNF α expression and activity is also highest in early atherosclerotic lesions.⁵⁵ For these reasons, we

delivered antisense inhibitors targeting RIPK1 to mice during the initiation phases of lesion formation, when we predicted RIPK1 would be at its highest level. Similar to TNF α and RIPK1 expression, NF- κ B expression has been linked to early events in the initiation of atherosclerosis, where it is expressed in SMCs and macrophages and is elevated in ECs in atherosclerosis-prone regions.^{56–58} Unlike in ECs,⁵⁹ the complete loss of NF- κ B activity in macrophages does not reduce atherosclerosis and, in fact, promotes necrotic core expansion attributable to massive cell death of macrophages.⁶⁰ This implies that, not unlike RIPK1, basal levels of NF- κ B are required to restrict uncontrolled cell death. In contrast, studies that use specific NF- κ B inhibitors find that turning down NF- κ B, but not completely inactivating it, reduces inflammatory lesions and protects against atherosclerosis.^{61,62} Our data agree with the notion that activation of the RIPK1-NF- κ B axis early in lesion formation is a key driver of atherogenesis, in particular, in ECs, but that the basal activity of this pathway is necessary to avoid uncontrolled cell death and necrosis within lesions. Although we did not investigate the cell-specific roles for RIPK1 in driving atherogenesis, we speculate that RIPK1 knockdown could beneficially impact atherosclerosis development through both lesional macrophages and vascular ECs, because both of these cell types are targeted by the ASOs used in this study. However, because complete loss of RIPK1 in barrier tissues leads to unrestricted cell death and exacerbates inflammation, the contribution of endothelial versus macrophage RIPK1 to atherosclerosis remains to be investigated.^{45,46}

The concept of therapeutic targeting of inflammation to reduce cardiovascular disease risk has now been validated with the recent results of the CANTOS trial, where an IL-1 β blocking antibody reduced adverse cardiovascular events by 15% in patients with low circulating LDL cholesterol.¹⁵ Likewise, the COLCOT trial showed a significant reduction with the anti-inflammatory compound colchicine in patients that had a previous myocardial infarction.¹⁶ This indicates that, even with appropriate cholesterol management, inflammatory pathways persist and can be blocked to further prevent disease progression. However, blocking IL-1 β led to a significant increase in lethal infections, likely because of the important role IL-1 β plays in the host response to pathogens. We found reduced macrophage secretion of IL-1 α and IL-1 β with RIPK1 ASO treatment. Both IL-1 β and IL-1 α , which are downstream of NF- κ B activation, directly contribute to atherosclerotic lesion formation in mice,⁵ and we find that levels of IL-1 α are decreased on RIPK1 inhibition in both the serum and the lesion. Although the maturation of pro-IL-1 β is dependent on NLRP3 inflammasome activation and caspase-1 activity,⁴ IL-1 α activation can be independent of these processes.⁵ We have consistently shown that the inhibition or deletion of RIPK3, downstream of RIPK1, in advanced atherosclerotic plaques

does not affect circulating IL-1 β yet reduces advanced lesion development.^{10,37} Moreover, recent studies have revealed a role for IL-1 β in the stabilization of atherosclerotic plaques by activation of SMC responses, further calling into question the need to develop alternative anti-inflammatory therapies without complete abrogation of IL-1 β activity.⁶³ Because RIPK1 expression is elevated directly in the plaque in both mice and humans, and antisense approaches like those used in our study can target lesion burden without systemic changes in IL-1 β , we argue that targeting RIPK1 may be better suited to reduce inflammation in the atherosclerotic plaque while leaving host innate immune defenses intact.

In summary, we find that RIPK1 expression is high in plaques that can be classified as early and less advanced, likely when inflammatory indices are also elevated. In vitro, proinflammatory M1 macrophages express higher levels of RIPK1 than both M0 and M2, and, as such, reducing RIPK1 gene expression leads to a reduction in NF- κ B gene activation and secretion of IL-1 α in vivo, which is a key driver of atherosclerosis. In *Apoe*^{-/-} mice fed a high cholesterol diet for 8 weeks, RIPK1 ASOs reduced lesion progression and macrophage accumulation in comparison with control mice. Together these data implicate RIPK1 as a hub of inflammatory gene activation directly in the atherosclerotic plaque and a potentially important future therapeutic target for residual inflammatory risk in patients with high risk of developing coronary and other vascular diseases.

ARTICLE INFORMATION

Received October 25, 2018; accepted October 23, 2020.

The Data Supplement is available with this article at <https://www.ahajournals.org/doi/suppl/10.1161/CIRCULATIONAHA.118.038379>.

Authors

Denuja Karunakaran¹ PhD; My-Anh Nguyen, PhD; Michele Geoffrion, BSc; Dianne Vreeken, MSc; Zachary Lister, MSc; Henry S. Cheng, PhD; Nicola Otte; Patricia Essebier, BSc; Hailey Wyatt, BSc; Joshua W. Kandiah, BSc; Richard Jung² MD; Francis J. Alenghat, MD, PhD; Ana Mompeon³ PhD; Richard Lee, PhD; Calvin Pan, PhD; Emma Gordon, PhD; Adil Rasheed, PhD; Aldons J. Lusis⁴ PhD; Peter Liu, MD; Ljubica Perisic Matic, PhD; Ulf Hedin, MD; Jason E. Fish⁵ PhD; Liang Guo, PhD; Frank Kolodgie, PhD; Renu Virmani⁶ MD; Janine M van Gils⁷ PhD; Katey J. Rayner⁸ PhD

Correspondence

Katey J. Rayner, 40 Ruskin Street, H4211, Ottawa, Ontario, K1Y4W7 Canada; or Denuja Karunakaran, Institute for Molecular Bioscience, Brisbane Qld 4072 Australia. Email krayner@ottawaheart.ca or denuja.karunakaran@gmail.com

Affiliations

University of Ottawa Heart Institute, Canada (D.K., M.-A.N., M.G., Z.L., H.W., J.W.K., R.J., A.M., A.R., P.L., K.J.R.). Leiden University Medical Center, The Netherlands (D.V., J.M.v.G.). Toronto General Research Hospital Institute, University Health Network, Department of Laboratory Medicine and Pathobiology, University of Toronto, Ontario, Canada (H.S.C.). Cardiology, Department of Medicine, University of Chicago, IL (F.J.A., J.E.F.). Cardiovascular Antisense Drug Discovery Group, Ionis Pharmaceuticals, Carlsbad, CA (R.L.). David Geffen School of Medicine, University of California Los Angeles (C.P., A.J.L.). Vascular Surgery Division, Department of Molecular Medicine and Surgery, Karolinska Institute,

Sweden (L.P.M.). CVPath Institute Inc., Gaithersburg, MD (L.G., F.K., R.V.). Department of Biochemistry, Microbiology and Immunology, University of Ottawa, Ontario, Canada (M.-A.N., K.J.R.). Institute for Molecular Bioscience, University of Queensland, St Lucia, Australia (D.K., N.O., P.E., E.G.).

Acknowledgments

The authors acknowledge the Animal Care and Veterinary Services at the University of Ottawa Heart Institute for their expertise; X. Zhao for her technical assistance, and University of Queensland Biological Resources. Dr Karunakaran, H. Wyatt, J.W. Kandiah, and Dr Mompeon performed *in vitro* assays. Dr Karunakaran, Dr Nguyen, M. Geoffrion, and Z. Lister performed the animal studies and analysis. Drs Jung, Alenghat, Guo, Kolodgie, Virmani, and Rayner performed human sample analysis. Dr Lee provided the antisense oligonucleotides. Drs Matic and Hedin contributed data from the BiKE Project (Biobank of Karolinska Endarterectomies). Drs Cheng and Fish performed gene expression analysis in *Ldlr*^{-/-} mice aortas. Drs Pan and Lusic performed analyses from the Hybrid Mouse Diversity Panel data set. Drs Vreeken and van Gils performed the endothelial cell studies. Drs Karunakaran and Rayner wrote the article with input from all authors.

Sources of Funding

This study was supported with funding from the following organizations: Canadian Institutes of Health Research (to Dr Rayner), National Institutes of Health (R01 HL119047 to Dr Rayner, HL147883 and HL144651 to Dr Lusic), European Research Area Network on Cardiovascular Diseases (to Dr Rayner and van Gils), National Psoriasis Foundation (to Dr Karunakaran) and the University of Queensland (to Dr Karunakaran) The BiKE Study was conducted with support from the Swedish Heart and Lung Foundation, the Swedish Research Council (K2009-65X-2233-01-3, K2013-65X-06816-30-4, and 349-2007-8703), Uppdrag Besegra Stroke (P581/2011-123), the Strategic Cardiovascular Programs of Karolinska Institutet and Stockholm County Council, the Stockholm County Council (ALF2011-0260 and ALF-2011-0279) and the Foundation for Strategic Research. Dr Matic is the recipient of fellowships from the Swedish Society for Medical Research and the Swedish Heart and Lung Foundation. Dr Gordon was supported by a National Health and Medical Research Council Project Grant (APP1158002) and an Australian Research Council Discovery Project (DP200100737). Dr Lusic was supported by le Fondation Leduc. Dr van Gils was supported by the Dutch Heart Foundation (2013T1127). Drs van Gils and Rayner were supported by the MiSS-CVD (European Research Area Network on Cardiovascular Diseases).

Disclosures

Dr Lee is an employee of Ionis Pharmaceuticals. The other authors have no other disclosures.

Supplemental Materials

Data Supplement Figures I–IV

REFERENCES

1. Tabas I, Lichtman AH. Monocyte-macrophages and T cells in atherosclerosis. *Immunity*. 2017;47:621–634. doi: 10.1016/j.immuni.2017.09.008
2. Tabas I, Bornfeldt KE. Macrophage phenotype and function in different stages of atherosclerosis. *Circ Res*. 2016;118:653–667. doi: 10.1161/CIRCRESAHA.115.306256
3. Collins T, Cybulsky MI. NF-kappaB: pivotal mediator or innocent bystander in atherogenesis? *J Clin Invest*. 2001;107:255–264. doi: 10.1172/JCI10373
4. Sheedy FJ, Grebe A, Rayner KJ, Kalantari P, Ramkhalawon B, Carpenter SB, Becker CE, Ediriweera HN, Mullick AE, Golenbock DT, et al. CD36 coordinates NLRP3 inflammasome activation by facilitating intracellular nucleation of soluble ligands into particulate ligands in sterile inflammation. *Nat Immunol*. 2013;14:812–820. doi: 10.1038/ni.2639
5. Freigang S, Ampenberger F, Weiss A, Kanneganti TD, Iwakura Y, Hersberger M, Kopf M. Fatty acid-induced mitochondrial uncoupling elicits inflammasome-independent IL-1 α and sterile vascular inflammation in atherosclerosis. *Nat Immunol*. 2013;14:1045–1053. doi: 10.1038/ni.2704
6. Crisby M, Kallin B, Thyberg J, Zhivotovskiy B, Orrenius S, Kostulas V, Nilsson J. Cell death in human atherosclerotic plaques involves both oncosis and apoptosis. *Atherosclerosis*. 1997;130:17–27. doi: 10.1016/s0021-9150(96)06037-6
7. Liu J, Thewke DP, Su YR, Linton MF, Fazio S, Sinensky MS. Reduced macrophage apoptosis is associated with accelerated atherosclerosis in low-density lipoprotein receptor-null mice. *Arterioscler Thromb Vasc Biol*. 2005;25:174–179. doi: 10.1161/01.ATV.0000148548.47755.22
8. Arai S, Shelton JM, Chen M, Bradley MN, Castrillo A, Bookout AL, Mak PA, Edwards PA, Mangelsdorf DJ, Tontonoz P, et al. A role for the apoptosis inhibitory factor AIM/Spalpa/Ap16 in atherosclerosis development. *Cell Metab*. 2005;1:201–213. doi: 10.1016/j.cmet.2005.02.002
9. Rayner KJ. Cell death in the vessel wall: the good, the bad, the ugly. *Arterioscler Thromb Vasc Biol*. 2017;37:e75–e81. doi: 10.1161/ATVBAHA.117.309229
10. Karunakaran D, Geoffrion M, Wei L, Gan W, Richards L, Shangari P, DeKemp EM, Beanlands RA, Perisic L, Maegdefessel L, et al. Targeting macrophage necroptosis for therapeutic and diagnostic interventions in atherosclerosis. *Sci Adv*. 2016;2:e1600224. doi: 10.1126/sciadv.1600224
11. Kasikara C, Doran AC, Cai B, Tabas I. The role of non-resolving inflammation in atherosclerosis. *J Clin Invest*. 2018;128:2713–2723. doi: 10.1172/JCI97950
12. Yurdagul A Jr, Doran AC, Cai B, Fredman G, Tabas IA. Mechanisms and consequences of defective efferocytosis in atherosclerosis. *Front Cardiovasc Med*. 2017;4:86. doi: 10.3389/fcvm.2017.00086
13. Baigent C, Blackwell L, Emberson J, Holland LE, Reith C, Bhalra N, Peto R, Barnes EH, Keech A, Simes J, et al; Cholesterol Treatment Trilists' (CTT) Collaboration. Efficacy and safety of more intensive lowering of LDL cholesterol: a meta-analysis of data from 170,000 participants in 26 randomised trials. *Lancet*. 2010;376:1670–1681. doi: 10.1016/S0140-6736(10)61350-5
14. Kingwell BA, Chapman MJ, Kontush A, Miller NE. HDL-targeted therapies: progress, failures and future. *Nat Rev Drug Discov*. 2014;13:445–464. doi: 10.1038/nrd4279
15. Ridker PM, Everett BM, Thuren T, MacFadyen JG, Chang WH, Ballantyne C, Fonseca F, Nicolau J, Koenig W, Anker SD, et al; CANTOS Trial Group. Anti-inflammatory therapy with canakinumab for atherosclerotic disease. *N Engl J Med*. 2017;377:1119–1131. doi: 10.1056/NEJMoa1707914
16. Tardif JC, Kouz S, Waters DD, Bertrand OF, Diaz R, Maggioni AP, Pinto FJ, Ibrahim R, Gamra H, Kiwan GS, et al. Efficacy and safety of low-dose colchicine after myocardial infarction. *N Engl J Med*. 2019;381:2497–2505. doi: 10.1056/NEJMoa1912388
17. Silke J, Rickard JA, Gerlic M. The diverse role of RIP kinases in necroptosis and inflammation. *Nat Immunol*. 2015;16:689–697. doi: 10.1038/ni.3206
18. Dondelinger Y, Darding M, Bertrand MJ, Walczak H. Poly-ubiquitination in TNFR1-mediated necroptosis. *Cell Mol Life Sci*. 2016;73:2165–2176. doi: 10.1007/s00018-016-2191-4
19. Moquin DM, McQuade T, Chan FK. CYLD deubiquitinates RIP1 in the TNF α -induced necrosome to facilitate kinase activation and programmed necrosis. *PLoS One*. 2013;8:e76841. doi: 10.1371/journal.pone.0076841
20. Cuny GD, Degtrev A. RIPK protein kinase family: atypical lives of typical kinases [published online July 27, 2020]. *Semin Cell Dev Biol*. doi: 10.1016/j.semcdb.2020.06.014. <https://www.sciencedirect.com/science/article/abs/pii/S1084952119302447>
21. Petrie EJ, Czabotar PE, Murphy JM. The structural basis of necroptotic cell death signaling. *Trends Biochem Sci*. 2019;44:53–63. doi: 10.1016/j.tibs.2018.11.002
22. Karunakaran D, Geoffrion M, Wei L, Gan W, Richards L, Shangari P, DeKemp EM, Beanlands RA, Perisic L, Maegdefessel L, et al. Targeting macrophage necroptosis for therapeutic and diagnostic interventions in atherosclerosis. *Sci Adv*. 2016;2:e1600224. doi: 10.1126/sciadv.1600224
23. Lin J, Li H, Yang M, Ren J, Huang Z, Han F, Huang J, Ma J, Zhang D, Zhang Z, et al. A role of RIP3-mediated macrophage necrosis in atherosclerosis development. *Cell Rep*. 2013;3:200–210. doi: 10.1016/j.celrep.2012.12.012
24. Nguyen MA, Karunakaran D, Geoffrion M, Cheng HS, Tandoc K, Perisic Matic L, Hedin U, Maegdefessel L, Fish JE, Rayner KJ. Extracellular vesicles secreted by atherogenic macrophages transfer microRNA to inhibit cell migration. *Arterioscler Thromb Vasc Biol*. 2018;38:49–63. doi: 10.1161/ATVBAHA.117.309795
25. Naylor AR, Rothwell PM, Bell PR. Overview of the principal results and secondary analyses from the European and North American randomised trials of endarterectomy for symptomatic carotid stenosis. *Eur J Vasc Endovasc Surg*. 2003;26:115–129. doi: 10.1053/ejvs.2002.1946
26. Perisic L, Aldi S, Sun Y, Folkersen L, Razuvaev A, Roy J, Lengquist M, Åkesson S, Wheelock CE, Maegdefessel L, et al. Gene expression signatures, pathways and networks in carotid atherosclerosis. *J Intern Med*. 2016;279:293–308. doi: 10.1111/joim.12448

27. Edgar R, Domrachev M, Lash AE. Gene Expression Omnibus: NCB1 gene expression and hybridization array data repository. *Nucleic Acids Res*. 2002;30:207–210. doi: 10.1093/nar/30.1.207
28. Ayari H, Bricca G. Identification of two genes potentially associated in iron-heme homeostasis in human carotid plaque using microarray analysis. *J Biosci*. 2013;38:311–315. doi: 10.1007/s12038-013-9310-2
29. Arking DE, Junttila MJ, Goyette P, Huertas-Vazquez A, Eijgelsheim M, Blom MT, Newton-Cheh C, Reinier K, Teodorescu C, Uy-Evanado A, et al. Identification of a sudden cardiac death susceptibility locus at 2q24.2 through genome-wide association in European ancestry individuals. *PLoS Genet*. 2011;7:e1002158. doi: 10.1371/journal.pgen.1002158
30. Berger SB, Kasparcova V, Hoffman S, Swift B, Dare L, Schaeffer M, Capriotti C, Cook M, Finger J, Hughes-Earle A, et al. Cutting edge: RIP1 kinase activity is dispensable for normal development but is a key regulator of inflammation in SHARPIN-deficient mice. *J Immunol*. 2014;192:5476–5480. doi: 10.4049/jimmunol.1400499
31. Sun X, He S, Wara AKM, Icli B, Shvartz E, Tesmenitsky Y, Belkin N, Li D, Blackwell TS, Sukhova GK, et al. Systemic delivery of microRNA-181b inhibits nuclear factor- κ B activation, vascular inflammation, and atherosclerosis in apolipoprotein E-deficient mice. *Circ Res*. 2014;114:32–40. doi: 10.1161/CIRCRESAHA.113.302089
32. Lusk AJ, Seldin MM, Allayee H, Bennett BJ, Civelek M, Davis RC, Eskin E, Farber CR, Hui S, Mehrabian M, et al. The Hybrid Mouse Diversity Panel: a resource for systems genetics analyses of metabolic and cardiovascular traits. *J Lipid Res*. 2016;57:925–942. doi: 10.1194/jlr.R066944
33. Bennett BJ, Davis RC, Civelek M, Orozco L, Wu J, Qi H, Pan C, Packard RR, Eskin E, Yan M, et al. Genetic architecture of atherosclerosis in mice: a systems genetics analysis of common inbred strains. *PLoS Genet*. 2015;11:e1005711. doi: 10.1371/journal.pgen.1005711
34. Cheng HS, Besla R, Li A, Chen Z, Shikatani EA, Nazari-Jahantigh M, Hammoutène A, Nguyen MA, Geoffrion M, Cai L, et al. Paradoxical suppression of atherosclerosis in the absence of microRNA-146a. *Circ Res*. 2017;121:354–367. doi: 10.1161/CIRCRESAHA.116.310529
35. Karunakaran D, Richards L, Geoffrion M, Barrette D, Gotfrit RJ, Harper ME, Rayner KJ. Therapeutic inhibition of miR-33 promotes fatty acid oxidation but does not ameliorate metabolic dysfunction in diet-induced obesity. *Arterioscler Thromb Vasc Biol*. 2015;35:2536–2543. doi: 10.1161/ATVBAHA.115.306404
36. Rayner KJ, Sheedy FJ, Esau CC, Hussain FN, Temel RE, Parathath S, van Gils JM, Rayner AJ, Chang AN, Suarez Y, et al. Antagonism of miR-33 in mice promotes reverse cholesterol transport and regression of atherosclerosis. *J Clin Invest*. 2011;121:2921–2931. doi: 10.1172/JCI57275
37. Meng L, Jin W, Wang X. RIP3-mediated necrotic cell death accelerates systemic inflammation and mortality. *Proc Natl Acad Sci USA*. 2015;112:11007–11012. doi: 10.1073/pnas.1514730112
38. Newton K. RIPK1 and RIPK3: critical regulators of inflammation and cell death. *Trends Cell Biol*. 2015;25:347–353. doi: 10.1016/j.tcb.2015.01.001
39. Sun X, Sit A, Feinberg MW. Role of miR-181 family in regulating vascular inflammation and immunity. *Trends Cardiovasc Med*. 2014;24:105–112. doi: 10.1016/j.tcm.2013.09.002
40. Dondelinger Y, Delanghe T, Rojas-Rivera D, Priem D, Delvaeye T, Bruggeman I, Van Herreweghe F, Vandenabeele P, Bertrand MJM. MK2 phosphorylation of RIPK1 regulates TNF-mediated cell death. *Nat Cell Biol*. 2017;19:1237–1247. doi: 10.1038/ncb3608
41. Jaco I, Annibaldi A, Lalaoui N, Wilson R, Tenev T, Laurien L, Kim C, Jamal K, Wicky John S, Liccardi G, et al. MK2 phosphorylates RIPK1 to prevent TNF-induced cell death. *Mol Cell*. 2017;66:698–710.e5. doi: 10.1016/j.molcel.2017.05.003
42. Menon MB, Gropengießer J, Fischer J, Novikova L, Deuretzbacher A, Lafera J, Schimmeck H, Czymbek N, Ronkina N, Kotlyarov A, et al. p38MAPK/MK2-dependent phosphorylation controls cytotoxic RIPK1 signalling in inflammation and infection. *Nat Cell Biol*. 2017;19:1248–1259. doi: 10.1038/ncb3614
43. Kelliher MA, Grimm S, Ishida Y, Kuo F, Stanger BZ, Leder P. The death domain kinase RIP mediates the TNF-induced NF- κ B signal. *Immunity*. 1998;8:297–303. doi: 10.1016/s1074-7613(00)80535-x
44. Zhang H, Zhou X, McQuade T, Li J, Chan FK, Zhang J. Functional complementation between FADD and RIP1 in embryos and lymphocytes. *Nature*. 2011;471:373–376. doi: 10.1038/nature09878
45. Dannappel M, Vlantis K, Kumari S, Polykratis A, Kim C, Wachsmuth L, Eftychi C, Lin J, Corona T, Hermance N, et al. RIPK1 maintains epithelial homeostasis by inhibiting apoptosis and necroptosis. *Nature*. 2014;513:90–94. doi: 10.1038/nature13608
46. Takahashi N, Vereecke L, Bertrand MJ, Duprez L, Berger SB, Divert T, Gonçalves A, Sze M, Gilbert B, Kouroula S, et al. RIPK1 ensures intestinal homeostasis by protecting the epithelium against apoptosis. *Nature*. 2014;513:95–99. doi: 10.1038/nature13706
47. Lalaoui N, Boyden SE, Oda H, Wood GM, Stone DL, Chau D, Liu L, Stoffels M, Kratina T, Lawlor KE, et al. Mutations that prevent caspase cleavage of RIPK1 cause autoinflammatory disease. *Nature*. 2020;577:103–108. doi: 10.1038/s41586-019-1828-5
48. Li Y, Führer M, Bahrami E, Socha P, Kludel-Dreszler M, Bouzidi A, Liu Y, Lehle AS, Magg T, Hollizeck S, et al. Human RIPK1 deficiency causes combined immunodeficiency and inflammatory bowel diseases. *Proc Natl Acad Sci USA*. 2019;116:970–975. doi: 10.1073/pnas.1813582116
49. Cuchet-Lourenço D, Eletto D, Wu C, Plagnol V, Papapietro O, Curtis J, Ceron-Gutierrez L, Bacon CM, Hackett S, Alsalem B, et al. Biallelic RIPK1 mutations in humans cause severe immunodeficiency, arthritis, and intestinal inflammation. *Science*. 2018;361:810–813. doi: 10.1126/science.aar2641
50. Yonekawa T, Gamez G, Kim J, Tan AC, Thorburn J, Gump J, Thorburn A, Morgan MJ. RIP1 negatively regulates basal autophagic flux through TFEB to control sensitivity to apoptosis. *EMBO Rep*. 2015;16:700–708. doi: 10.15252/embr.201439496
51. Green DR. Another face of RIPK1. *EMBO Rep*. 2015;16:674–675. doi: 10.15252/embr.201540470
52. Levin MC, Jirholt P, Wramstedt A, Johansson ME, Lundberg AM, Trajkovska MG, Ståhlman M, Fogelstrand P, Brisslert M, Fogelstrand L, et al. Rip2 deficiency leads to increased atherosclerosis despite decreased inflammation. *Circ Res*. 2011;109:1210–1218. doi: 10.1161/CIRCRESAHA.111.246702
53. Shimada K, Chen S, Dempsey PW, Sorrentino R, Alsabeh R, Slepkin AV, Peterson E, Doherty TM, Underhill D, Crother TR, et al. The NOD/RIP2 pathway is essential for host defenses against *Chlamydia pneumoniae* lung infection. *PLoS Pathog*. 2009;5:e1000379. doi: 10.1371/journal.ppat.1000379
54. Sukumaran B, Ogura Y, Pedra JH, Kobayashi KS, Flavell RA, Fikrig E. Receptor interacting protein-2 contributes to host defense against *Anaplasma phagocytophilum* infection. *FEMS Immunol Med Microbiol*. 2012;66:211–219. doi: 10.1111/j.1574-695X.2012.01001.x
55. Xiao N, Yin M, Zhang L, Qu X, Du H, Sun X, Mao L, Ren G, Zhang C, Geng Y, et al. Tumor necrosis factor- α deficiency retards early fatty-streak lesion by influencing the expression of inflammatory factors in apoE-null mice. *Mol Genet Metab*. 2009;96:239–244. doi: 10.1016/j.ymgme.2008.11.166
56. de Winther MP, Kanters E, Kraal G, Hofker MH. Nuclear factor kappaB signaling in atherogenesis. *Arterioscler Thromb Vasc Biol*. 2005;25:904–914. doi: 10.1161/01.ATV.0000160340.72641.87
57. Brand K, Page S, Rogler G, Bartsch A, Brandl R, Knuechel R, Page M, Kaltschmidt C, Baeuerle PA, Neumeier D. Activated transcription factor nuclear factor-kappa B is present in the atherosclerotic lesion. *J Clin Invest*. 1996;97:1715–1722. doi: 10.1172/JCI118598
58. Hajra L, Evans AI, Chen M, Hyduk SJ, Collins T, Cybulsky MI. The NF- κ B signal transduction pathway in aortic endothelial cells is primed for activation in regions predisposed to atherosclerotic lesion formation. *Proc Natl Acad Sci USA*. 2000;97:9052–9057. doi: 10.1073/pnas.97.16.9052
59. Gareus R, Kotsaki E, Xanthouleas S, van der Made I, Gijbels MJ, Kardakaris R, Polykratis A, Kollias G, de Winther MP, Pasparakis M. Endothelial cell-specific NF- κ B inhibition protects mice from atherosclerosis. *Cell Metab*. 2008;8:372–383. doi: 10.1016/j.cmet.2008.08.016
60. Kanters E, Pasparakis M, Gijbels MJ, Vergouwe MN, Partouns-Hendriks I, Fijneman RJ, Clausen BE, Förster I, Kockx MM, Rajewsky K, et al. Inhibition of NF- κ B activation in macrophages increases atherosclerosis in LDL receptor-deficient mice. *J Clin Invest*. 2003;112:1176–1185. doi: 10.1172/JCI118580
61. Zhang Y, Yang X, Bian F, Wu P, Xing S, Xu G, Li W, Chi J, Ouyang C, Zheng T, et al. TNF- α promotes early atherosclerosis by increasing transcytosis of LDL across endothelial cells: cross-talk between NF- κ B and PPAR- γ . *J Mol Cell Cardiol*. 2014;72:85–94. doi: 10.1016/j.jmcc.2014.02.012
62. Mallavia B, Recio C, Oguiza A, Ortiz-Muñoz G, Lizaro I, Lopez-Parra V, Lopez-Franco O, Schindler S, Depping R, Egido J, et al. Peptide inhibitor of NF- κ B translocation ameliorates experimental atherosclerosis. *Am J Pathol*. 2013;182:1910–1921. doi: 10.1016/j.ajpath.2013.01.022
63. Gomez D, Baylis RA, Durgin BG, Newman AAC, Alencar GF, Mahan S, St Hilaire C, Müller W, Waisman A, Francis SE, et al. Interleukin-1 β has atheroprotective effects in advanced atherosclerotic lesions of mice. *Nat Med*. 2018;24:1418–1429. doi: 10.1038/s41591-018-0124-5